Sub-harmonic Entrainment of Cortical Gamma Oscillations to Deep Brain Stimulation in Parkinson's Disease: Predictions and Validation of a Patient-Specific Nonlinear Model

James J. Sermon[1,2†], Maria Olaru[3†], Juan Anso[3], Simon Little[4], Rafal Bogacz[2], Philip A. Starr[3‡], Timothy Denison[1,2‡], Benoit Duchet[2‡*]

1 Institute of Biomedical Engineering, Department of Engineering Science, University of Oxford, Oxford, UK

2 MRC Brain Networks Dynamcis Unit, Nuffield Department of Clinical Neurosciences, University of Oxford, Oxford, UK

3 Department of Neurological Surgery and Weill Institute for Neurosciences, University of California San Francisco, San Francisco, California, USA

4 Department of Neurology, University of California San Francisco, San Francisco, California, USA

†These authors contributed equally to this work.

‡These authors share senior authorship.

*Corresponding author at: MRC Brain Network Dynamics Unit, University of Oxford, Mansfield Road, Oxford OX1 3TH, UK. Email address: benoit.duchet@ndcn.ox.ac.uk

Abstract

Objectives: The exact mechanisms of deep brain stimulation (DBS) are still an active area of investigation, in spite of its clinical successes. This is due in part to the lack of understanding of the effects of stimulation on neuronal rhythms. Entrainment of brain oscillations has been hypothesised as a potential mechanism of neuromodulation. Better understanding entrainment might further inform existing methods of continuous DBS, and help refine algorithms for adaptive methods. The purpose of this study was to demonstrate that cortical finely-tuned gamma oscillations around 75Hz being entrained at 65Hz during 130Hz DBS in patients with Parkinson's disease (PD) are consistent with 1:2 entrainment, a special case of sub-harmonic entrainment predicted by synchronisation theory. Furthermore, we looked to predict stimulation parameters that would result in 1:2 entrainment.

Materials and Methods: We fit a coupled neuronal population model to selected features characterising a PD patient's off-stimulation finely-tuned gamma rhythm recorded through electrocorticography.

Results: Our model predicts the regions of entrainment (Arnold tongues) in the stimulation frequency/amplitude space. We show that the resulting neural circuit model fitted to patient data exhibits 1:2 entrainment when stimulation is provided at 130Hz. Furthermore, we verify keys features of the 1:2 Arnold tongue with follow-up recordings from the same patient, such as the loss of 1:2 entrainment beyond a certain stimulation amplitude.

Conclusion: Our results reveal that periodic DBS in patients may lead to nonlinear patterns of neuronal entrainment across stimulation parameters, and that these responses can be predicted by modelling. Should entrainment prove to be an important mechanism of therapeutic stimulation, our modelling framework may reduce the parameter space that clinicians must consider when programming devices for optimal benefit.

Introduction

Deep Brain Stimulation (DBS) is a form of invasive neuromodulation, where electrical impulses are delivered to specific brain regions by implanted electrodes. In the context of Parkinson's disease (PD), DBS is primarily used to alleviate motor symptoms when pharmaceutical measures do not provide therapeutic benefit. While a diverse range of effects of DBS have been observed in both behaviour and neuronal rhythms, the exact mechanisms underlying these responses are not fully understood.

Activity in the gamma band (approximately 30 to 100Hz) has become a target for neuromodulation as it is associated with various cognitive performance features [1] as well as motor control [2]. Invasive recordings of the basal ganglia in PD have revealed gamma oscillations at 60-90Hz in patients on antiparkinsonian medications [3, 4]. These have been thought to represent a "prokinetic" brain rhythm, in contrast to "antikinetic" beta rhythms (13-30Hz). Recently, prominent finely-tuned gamma oscillations (a narrowband gamma activity [5]) at 60-90Hz have been found during invasive recordings from motor cortical areas in PD [6, 7, 8], and may be associated with dyskinesias. Additionally, similar cortical oscillations have been observed in rat models of dyskinesia [9, 10].

Stimulation targeting gamma band activity has been shown to improve motor symptoms in PD by a comparable scale to high-frequency stimulation, while this was not observed for stimulation at theta and beta frequencies [11]. In another study, transcranial alternating current stimulation (tACS) at gamma frequency was observed to increase motor velocity in PD, while tACS at beta frequency saw it decrease [12]. It was hypothesised that entrainment (specifically 1:1 entrainment, as depicted in Fig 1B) of both gamma and beta oscillations would explain this observation by enhancing "prokinetic"

and "antikinetic" rhythms, respectively. This suggests that gamma entrainment may have potential to modulate PD-associated motor symptoms.

Further evidence of cortical gamma entrainment is provided by observations of modulated cortical gamma rhythms in response to stimulation. The ability to entrain gamma rhythms at stimulation frequency has been shown through varying visual stimulation at gamma frequency in the Macaque V1 [13]. Cross-frequency coupling of cortical finely-tuned gamma to the stimulation frequency has also been observed in PD patients with Subthalamic Nucleus (STN) DBS [14]. Additionally, a shifted finely-tuned gamma peak has been noted in the motor cortex in response to high-frequency (130Hz) DBS of the STN [6, 15, 8, 16]. The gamma peak, off-stimulation between 75 and 80Hz, locks to the half harmonic of stimulation (see Fig 1), corresponding to 1:2 entrainment. This half harmonic lock suggests that modulation goes beyond solely entraining rhythms at the frequency being applied or suppressing them like an information blockade. Currently, there is no theoretical understanding of 1:2 gamma entrainment in PD and generally no framework to predict the occurrence of specific entrainment regimes in response to brain stimulation.

In this study, we look to set up a pathway to predict sub-harmonic entrainment of brain rhythms by DBS in PD patients, using a model-based approach that is informed by data. We postulate that by constraining the parameters of a neuronal population model to patient data, it will be possible to predict stimulation parameters that lead to 1:2 gamma entrainment for subjects with off-stimulation gamma rhythms. We provide a theoretical introduction to 1:2 gamma entrainment using the simplest model of a neural oscillator receiving periodic stimulation, the sine circle map. However, the sine circle map cannot be fitted to patient data. Hence, we develop a patient specific approach by showing that the Wilson-Cowan model, a neural population model, is capable of replicating off-stimulation features of a finely-tuned gamma rhythm when fitted to electrocorticography (ECoG) data from a patient with PD. The fitted-model is capable of predicting the regions of 1:2 entrainment in the stimulation parameter (frequency and amplitude) space. We proceed to verify key features of the 1:2 entrainment region with follow-up recordings from the same patient. Lastly, these results are discussed and the implications are highlighted for future stimulation therapies.

Materials and methods

Rotation Number and Arnold Tongues

The frequency locking behaviour of a rhythm to external stimulation across stimulation frequency and amplitude can be described by frequency-locking regions called Arnold tongues [17]. Frequency

locking is observed when a rotation number of the form p:q, where p and q are coprime integers, is maintained for several stimulation periods. In general, the rotation number may not be a ratio of integers, and corresponds to the average number of oscillatory cycles achieved by the rhythm between two periodic pulses of the driving stimulation. This is calculated as

$$\frac{\theta_N - \theta_0}{2\pi N}, \tag{1}$$

where θ_N is the phase after N stimulation pulses (in this study, N > 50) and θ_0 is the initial phase. Previously, Arnold tongues have been used to describe 1:1 entrainment in response to noninvasive neuromodulation [18, 19, 20, 21]. Depending on the system considered and the stimulation waveform, Arnold tongues can theoretically exist for various rotation numbers, including p:q with large p and/or q. However, in real systems, often only the tongues of the most stable rotation numbers, corresponding to low p and q values, will be observed. Arnold tongues often have different shapes for different dynamical systems. Generally, an Arnold tongue expands in width across larger frequency ranges as stimulation amplitude increases. This continues up until an amplitude where the region may share stability with another frequency-locking ratio or lose stability altogether.

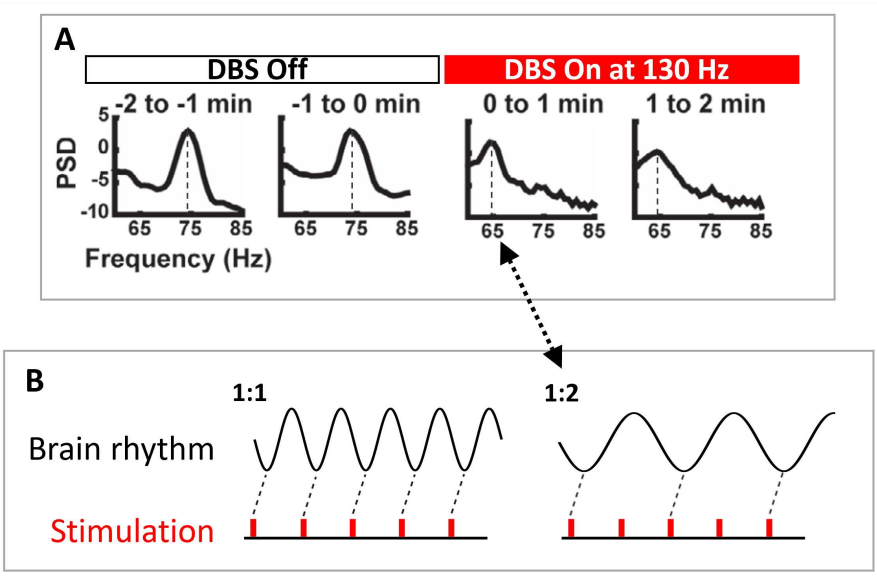

Figure 1: Prior human recordings demonstrate 1:2 entrainment of cortical gamma rhythms from subcortical stimulation. (A) PSD of gamma band activity before and during DBS to the STN at 130Hz. In the DBS Off state, a natural ∼75Hz gamma rhythm can be observed. This is entrained at 65Hz during the following two minutes of DBS On at 130Hz. (B) 1:1 entrainment = one stimulation pulse per brain rhythm cycle and a rotation number of 1, 1:2 entrainment = two stimulation pulses per brain rhythm cycle and a rotation number of 0.5. Hence, during 1:2 entrainment, the brain rhythm locks to a frequency of half that from the external stimulation. This corresponds to the DBS On state of panel A. Panel A is edited from [6].

Sine Circle Map

The sine circle map is the simplest model that describes the influence of periodic stimulation on an oscillator and can provide a first level description of gamma entrainment during 130Hz stimulation. The model stroboscopically observes the phase, θ, of a single oscillator of natural frequency f_0, periodically stimulated at frequency f_s and stimulation intensity, A_s. The map between the oscillator phase right after stimulation pulse i and its phase right after stimulation pulse $i+1$ is given by

$$\theta_{i+1} = \theta_i + 2\pi(f_0/f_s) + \mathrm{A}_s\mathrm{PRC}(\theta_i),$$

where PRC denotes the oscillator phase response curve and describes the change in the oscillator phase as a function of the stimulation phase. For the sine circle map, the PRC is given by $\mathrm{PRC}(\theta) = \sin(\theta)$.

While the sine circle map can provide a first level description of gamma entrainment, its simplicity results in significant limitations. Firstly, as the oscillator stays on the unit circle, there is no variable amplitude of oscillations. This makes anything more than analysis of a single neuronal unit unreliable. Secondly, the sine circle map only represents a single oscillator. Therefore it is difficult to draw comparisons to ECoG signals that arise from interacting populations of neurons. Thirdly, it is known that pulse shape impacts entrainment behaviour; however, as the sine circle map is stroboscopic, realistic pulses cannot be used. Hence, a model which captures the interaction of neurons, is representative of larger neuronal populations and for which realistic pulse shapes can be used would be more suitable. A model such as the Wilson-Cowan model would provide this.

Wilson-Cowan Model

The Wilson-Cowan model is well-suited to fit population-level brain recordings. The model is a heuristically derived mean-field model describing interacting neuronal populations [22, 23] and, hence, is a natural choice to represent ECoG recordings. The Wilson-Cowan model has been used in the analysis of neuronal responses to periodic and varying stimulation [24, 25, 26, 27, 28] and in theoretical studies of entrainment [29, 30]. Additionally, the model has been used in the analysis of resonances [31], as well as in the communication of information [32]. The Wilson-Cowan model has a limited number of model parameters which make it feasible to constrain the model without over-fitting. Despite the relatively small number of parameters, it is also able to capture a wide variety of dynamics [33, 34, 29].

We use the two-population Wilson-Cowan model to represent excitatory and inhibitory cortical populations with reciprocal connections (see Fig 2). The model can be used to predict the interactions of large groups of neurons and outputs the activity of excitatory and inhibitory populations. The

population activities are denoted by E and I, respectively, and are proportional to the firing rate of that population's neurons. Stochastic differential equations describe the evolution of E and I as

$$dE = \frac{1}{\tau_E}(-E + f(\eta_E + \omega_{EE}E + \omega_{IE}I))dt + \zeta dW_E$$
$$dI = \frac{1}{\tau_I}(-I + f(\eta_I + \omega_{EI}E) + A_{stim}(t))dt + \zeta dW_I$$
$$f(x) = \frac{1}{1 + e^{-b(x-1)}}.$$

These interactions are weighted by coupling strength, ω_{12} (going from population one to population two), and occur through a sigmoid function, $f(x)$, of steepness coefficient b. τ_E and τ_I represent the time constants of the excitatory and inhibitory populations respectively. η_E and η_I are the constant inputs to the respective populations. Stochasticity is introduced to the model through Wiener processes, W_E and W_I, with noise standard deviation denoted by ζ. Noise is required to reproduce the off-stimulation data, which is characterised by bursts of activity rather than perfectly periodic dynamics (see Fig 4D).

It is unclear whether stimulation of the external globus pallidus (GPe) has a net inhibitory or excitatory effect on the cortex. Connections via the thalamus likely have an excitatory effect on the cortex [35]. However, there also exist direct projections from cholinergic neurons in the GPe which have a solely GABAergic effect on the cortex [36]. Hence, while both inhibitory and excitatory projections exist from the GPe to the cortex, in this study we focus on the direct connection and apply periodic high-frequency stimulation, $A_{stim}(t)$, to the inhibitory population. However, we also consider stimulation applied to the excitatory population in Supplementary Data section 2.5. Stimulation is applied directly, not through the sigmoid function, as this provides a greater wealth of dynamics by avoiding saturation effects [28].

Data Collection

Cortical data off-stimulation were collected to fit the Wilson-Cowan model. On-stimulation data at variable stimulation frequencies and amplitudes were then used to compare and validate predictions from the fitted model. Human neural data were collected from a 64 year old female who had DBS implantation for motor fluctuations and medically intractable tremor, 13 years after onset of motor signs. The patient was diagnosed with idiopathic Parkinson's Disease and bilaterally implanted with the Medtronic Summit RC+S bidirectional neural interface (clinicaltrials.gov identifier

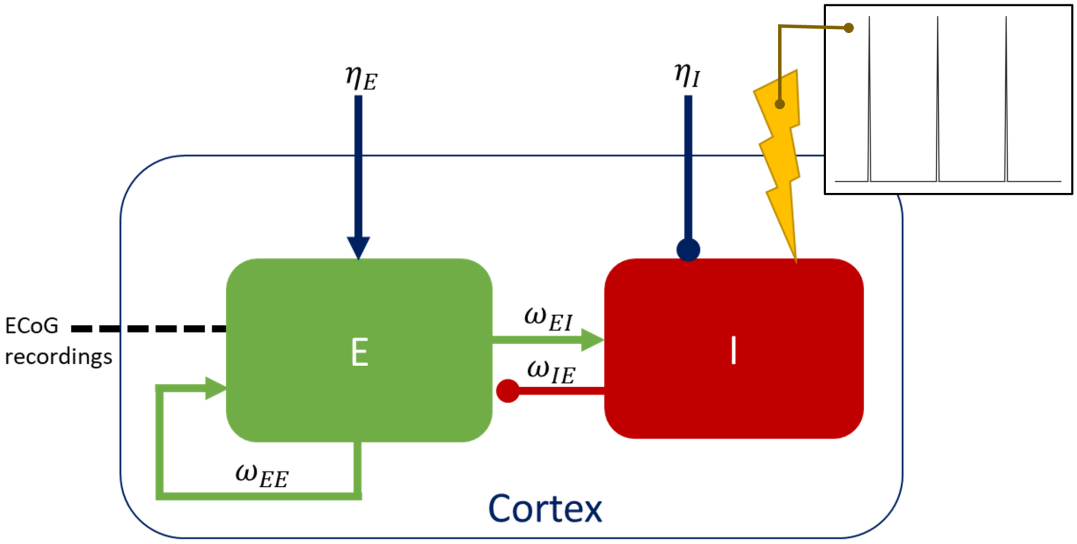

Figure 2: The two-population Wilson-Cowan model. Stimulation is applied to the inhibitory population (I) and data recorded from the excitatory population (E). The weights of the three connections present in this model are ω_{EI}, the weight of the excitatory effect on the inhibitory population, ω_{IE}, the weight of the inhibitory effect on the excitatory population, and ω_{EE}, the weight of the self excitatory effect. Additionally, there are external inputs, η_E and η_I, to each population. The insert displays the single time step stimulation pulse with no recharge used throughout study.

NCT03582891, USA FDA investigational device exemption number 180097, IRB number 18-24454), quadripolar cylindrical leads in the pallidal nuclei, and subdural paddle-type leads over the primary motor cortex, Figs 3A1-3. She had been chronically treated with antiparkinsonian medications, at a levodopa equivalent dose of 1083 mg/day at the time of surgery. Her preoperative unified Parkinson's disease rating scale (UPDRS) part 3 score was 89 twelve hours off of medication, improving by 53% in the on-medication state. The active contact array was localised in the globus pallidus (GP) using microelectrode recording (MER) mapping of single-unit cells to traverse the postero-lateral regions of the external globus pallidus (GPe) and internal globus pallidus (GPi), Fig 3A1. Localisation of contacts was further confirmed by computationally fusing a postoperative CT scan to the preoperative planning MRI scan, Figs 3A2-3. Prior to the initiation of standard therapeutic pallidal stimulation, we recorded four-channel local field potentials of the cortical and pallidal sites of each hemisphere across a month-long period. The data used for the fitting process was streamed from the patient wirelessly during normal activities of daily living, on their usual schedule of antiparkinsonian medication. The recording methods and data processing were similar to those described in Gilron et al. [8]. After ten months of continuous pallidal stimulation at 130Hz or 150 Hz with left hemisphere stimulation from contact two and right-hemisphere stimulation from contacts one and two, we conducted a follow-up in-clinic recording session to validate some of the model predictions and explore the DBS parameter space while the patient was on her usual antiparkinsonian medications. In this session, we cycled

through stimulation frequencies ranging 130-160Hz and stimulation amplitudes ranging 0-6.5mA under the guidance of a movement disorders neurologist. The patient was stimulated with a 90μs pulse width and an equivalent length "active recharge", where recharge is defined in Supplementary Data section 2.2. We recorded from two sensing contacts, +8-9 post-central sulcus, +10-11 pre-central sulcus, shown in Fig 3A3. Each trial of the data collection session consisted of a fixed frequency-amplitude pairing with a minimum 30-second duration and a 15-second inter-trial interval. We excluded data from the right hemisphere due to challenges interpreting data from dual stimulating contacts (contacts 1 and 2, using the subcortical contact numbering shown in Fig 3A1), while the left hemisphere was only stimulated by a single contact (contact 2).

Fitting Process

To fit the parameters of our Wilson-Cowan model, we processed the month-long off-stimulation recording to obtain data features for the model optimisation. We separated the off-stimulation sessions into epochs with a minimum of 30 seconds of continuous and uninterrupted recordings. The epoch used for the fitting process was selected by identifying the epoch with the most prominent gamma peak within the frequency range 72-78Hz, the approximate average of the overall dataset. From this epoch, three features were selected for the purposes of fitting the model; the power spectral density (PSD), the envelope PSD and the envelope probability density function (PDF), as shown in Fig 3B1-3. The envelope is the modulus of the analytic signal and refers to a curve that traces the upper bound of the signal, providing a measure of the oscillation's amplitude. These features were selected to provide a representation of the signal and its envelope in the frequency domain, as well as a representation of the statistics of the envelope in the time domain. We demonstrate that there is little correlation between the three features mentioned here and that all three features are required to capture the full dynamics of the data in Supplementary Data section 1.1. Fitting to off-stimulation features ensured that any presence of 1:2 entrainment is not predetermined, as would have been provided by a fit to on-stimulation data.

Model parameters were then optimised to best match the selected data features (Fig 3B1-3). This process follows a fitting methodology similar to [28, 37]. It begins by generating random sets of parameters, and selecting parameter sets with a PSD broadly similar to that of the data (the first loop of Fig 3C), i.e. with a gamma peak between 70 to 80Hz. This improves the computational efficiency of the parameter fitting and the overall duration of the optimisation. Accepted parameters enter an optimisation loop using the patternsearch function of Matlab2020b, which minimises the cost function (see Supplementary Data section 1.2) capturing the distance between model and data features (the

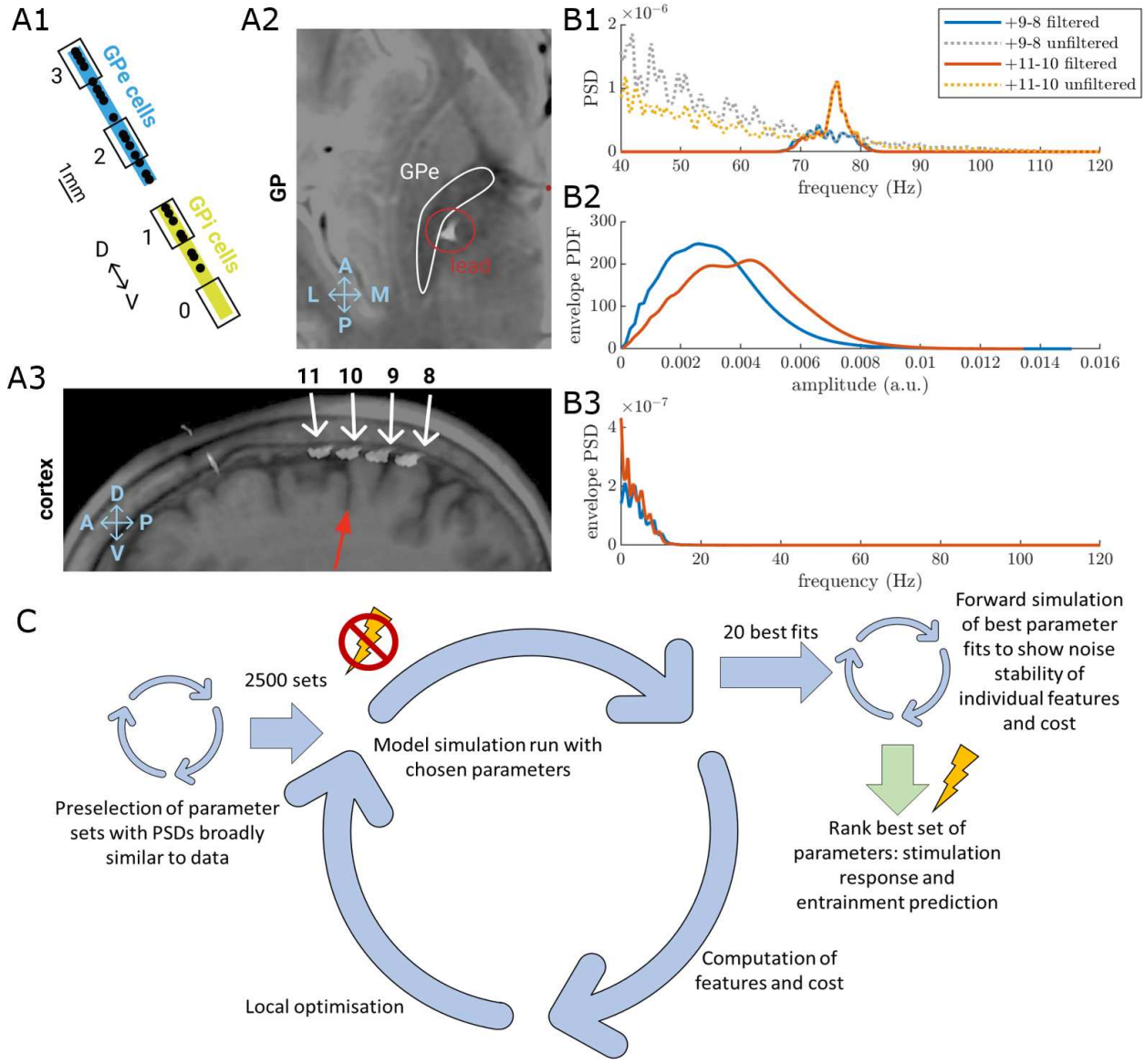

Figure 3: Use of prestimulation human neural recordings to fit Wilson-Cowan model parameters. (A1-3) Left hemisphere lead localisation. (A1) globus pallidus (GP) contact localisation (black numbered rectangles) with respect to the boundaries of the internal globus pallidus (yellow) and external globus pallidus (GPe) (blue) as defined by micro-electrode recording mapping of single-unit cells (black dots). (A2-3) Localization of contacts with a postoperative CT scan that is computationally fused with the preoperative planning MRI scan. (A2) GP lead on an axial T2-weighted MRI, which visualises the GP as regions of T2 hypointensity (GPe highlighted by a white contour). (A3) Quadripolar subdural paddle lead on sagittal T1-weighted MRI shows the relationship between the central sulcus (red arrow) and contacts (white numbered arrows).(B1-3) The three data features, power spectral density (PSD) (B1), envelope probability density function (PDF) (B2) and envelope PSD (B3), for the selected epoch, based on the gamma peak height in the cortical 9-8 and 11-10 contact. The features shown are from the cortical contacts as labelled in Panel A3. The orange and blue lines display the band-pass filtered cortical signals between 72Hz and 78Hz. The yellow and grey dotted line in the PSD plot shows the unfiltered signal which, for the 11-10 contact, still displays the finely-tuned gamma peak seen in the filtered data. The fitting is based off the filtered data from the 11-10 contact. (C) The optimisation pathway for fitting the model to off-stimulation data. This process is broken down into three main loops, as discussed in the *Fitting Process* section. Once a fitted set of model parameters is obtained we are able to make predictions for the neuronal population responses in the on-stimulation state.

second loop of Fig 3C). We run this optimisation to obtain approximately 2500 parameter sets fitted to the 30 seconds of off-stimulation data, each corresponding to a different local minimum of the cost function. From the resulting fits, we select the 20 with the greatest R^2 values and perform further simulations to refine the ranking of cost. As the model includes stochasticity, we also make sure that the optimal model parameter selections are robust to noise (the third loop of Fig 3C), more details can be found in Supplementary Data section 1.3. The top-ranked fit is then selected based on these simulations. We don't expect overfitting to be an issue given that we are fitting to off stimulation data, where there is no entrainment in the signal. Predictions of the response to external stimuli are then be made by introducing stimulation to the off-stimulation fitted model.

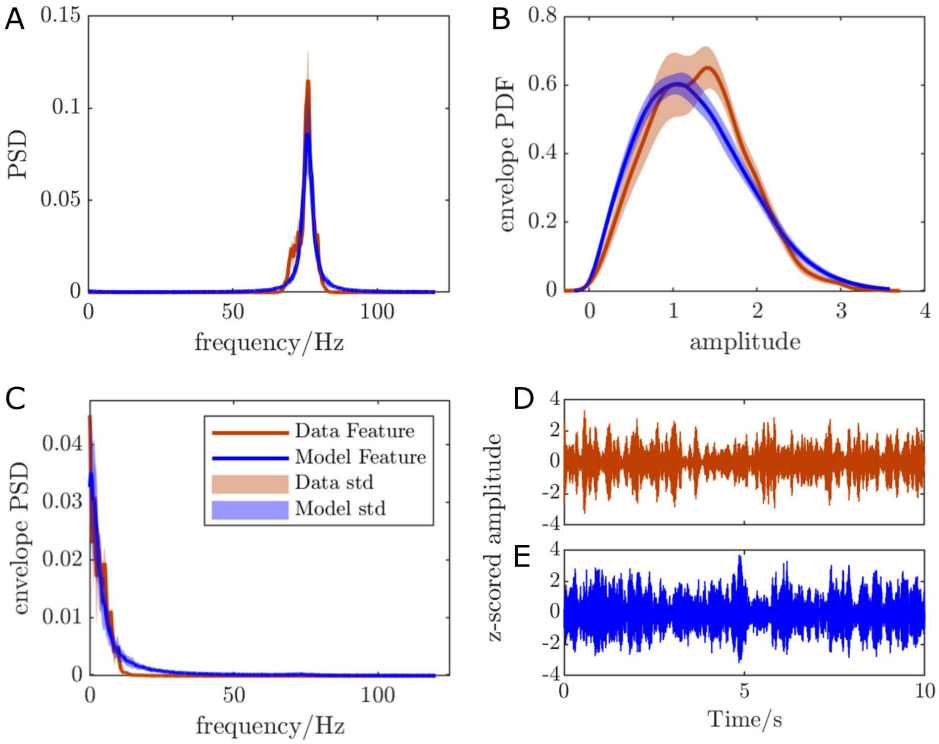

Figure 4: Comparison of the data features and the features of the best ranked model parameter set. $R^2 = 0.944$ on average across 50 simulations lasting 100 seconds each.The model closely matches the data PSD (A), envelope PDF (B), and envelope PSD (C). (D-E) Comparison of the band-passed, z-scored, off-stimulation time series from patient data and the model excitatory population time series data.

Providing Stimulation and Entrainment Analysis in the Model

The stimulation pulse provided throughout the majority of the modelling work in this study, unless mentioned otherwise, is a single time step positive pulse with no recharge (see the insert in Fig 2). This stimulation pulse was chosen for simplicity. Different recharge lengths and stimulation waveforms are explored in Supplementary Data sections 2.2 and 2.3. In the presence of stimulation, the rotation number is calculated using equation 1 where θ_i is taken as the unwrapped Hilbert phase of the

excitatory population activity over i stimulation pulses. This was calculated over 50 stimulation cycles and averaged over five repeats at each stimulation parameter.

The PSD of the model output with stimulation applied was calculated using Welch's PSD estimate over the same number of stimulation cycles and repeats as the rotation number. The peak PSD was calculated as the maximum power in the 0 to 200Hz frequency range.

Entrainment Analysis of the ECoG Recordings

The PSD of the data was calculated in a similar way to that of the model, using Welch's PSD estimate. Only frequencies recorded within the 50 to 120Hz range were considered when finding the peak power. To calculate the rotation number for a particular stimulation setting, the frequency of the maximum PSD power was divided by the stimulation frequency. Only rotation numbers of 0.5 ± 0.05 were considered to have resulted in 1:2 entrainment and marked by a circle in Fig 5E. However, Fig 5E remains unchanged when the tolerance on rotation numbers resulting in 1:2 entrainment is reduced to 0.5 ± 0.005.

Results

1:2 Entrainment During High-Frequency DBS is Predicted by the Sine Circle Map

Gamma entrainment during high-frequency DBS is predicted by even the simplest model that describes the influence of periodic stimulation on a neural oscillator, the sine circle map. In particular, we are able to observe a 1:2 Arnold tongue (Fig 5A), which predicts 1:2 entrainment for a 75Hz oscillator at 130Hz stimulation. There exists a specific range of stimulation amplitudes for which we would expect to see 1:2 entrainment of the oscillator at a resultant frequency of 65Hz. This is in agreement with the observations by Swann et al. [6, 15] and provides theoretical grounds for expecting 1:2 entrainment during high-frequency stimulation. However, the sine circle map only models a single oscillator (in this case a single neuron) responding to a periodic stimulus. We therefore turn to an interacting neural populations model that is fitted to patient data to predict stimulation parameters that lead to 1:2 entrainment.

Prediction of 1:2 Entrainment Using a Fitted Wilson-Cowan Model

The Wilson-Cowan model, fitted to the patient's pre-stimulation cortical data, oscillates at a fixed natural frequency of 75Hz in the absence of stimulation (shown in Fig 4A). This top ranked model parameter set (found in Supplementary Data Table 1.1) had an average R^2 value of 0.944 across 50

simulations, with good fits across all three features (Fig 4).

In the presence of low amplitude stimulation, the model displays a 1:2 tongue around a stimulation frequency of 150Hz (twice the natural frequency of the interacting populations). This is shown by the blue-green 1:2 tongue in Fig 5B, which corresponds to a constant rotation number of 0.5. When stimulation is provided at 130Hz (indicated by the black line), the excitatory population is entrained at 65Hz for a range of stimulation amplitudes. The 1:2 tongue is left leaning and stems from twice the natural frequency of the model, i.e. from 150Hz. This left lean suggests that there exist more parameters around 130Hz for which 1:2 entrainment would also be observed.

The left lean of the 1:2 tongue does not vary depending on whether stimulation is applied to the inhibitory population or the excitatory population (see Supplementary Data section 2.5), even though the decision was made to apply it to the inhibitory population. The 1:2 entrainment region exhibits a left lean regardless of whether the stimulation being applied is in the form of a single time step pulse train, pulse trains with various recharge durations or more complicated waveforms (see Supplementary Data sections 2.2 and 2.3).

The fitted Wilson-Cowan model also predicts that the highest spectral peaks will occur at the lowest frequencies for which 1:2 entrainment arises, as seen in Figs 5C-D.

Validation of Model Predictions in Human Patient During Chronic Therapeutic Stimulation

The presence of 1:2 entrainment at variable stimulation parameters was investigated in follow-up recordings for the same patient as the Wilson-Cowan model was fitted to (see recording details in the *Data Collection* section). These data were only examined following the core predictions from the model.

The data show a region of stimulation parameters for which 1:2 entrainment can be observed (Fig 5E) and appears to exhibit a similar shape to the Wilson-Cowan model predictions, as shown in Fig 5B. While 1:2 entrainment was seen for amplitudes greater than 5.5mA for 140 and 130Hz, it was lost for 150Hz. Hence, the 1:2 tongue has an approximate left lean from this set of data with 1:2 entrainment being maintained at higher amplitudes for lower frequencies of stimulation.

Comparing the predictions of entrained peak power in Fig 5D to the data collected provides further support for the fitted model. The data validate the model's prediction of highest power for the lower frequencies within the 1:2 tongue. Changing stimulation parameters from 130Hz, 6.5mA to 150Hz, 5mA results in a drop in entrained peak power, as indicated by the colourscale in Fig 5E. This is a change that reflects a fundamental difference in the resulting entrained activity, more than the

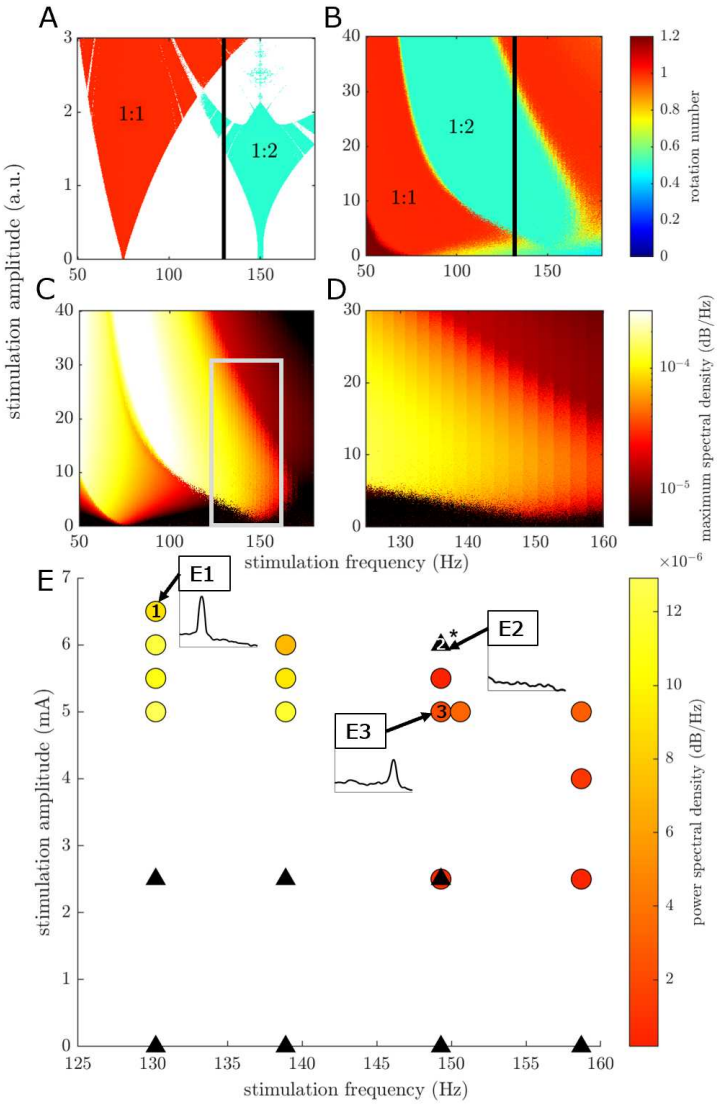

Figure 5: Testing model predictions of a cortical circuit's response to an external stimulus using human neural data during neurostimulation. Stimulation frequency is the horizontal axis for all panels, while stimulation amplitude is the vertical axis for all panels. Stimulation amplitude has arbitrary units (a.u.) for all model panels (A,B,C and D) and is in mA for the data panel (E). Panels A and B have a jet-scaled colourbar indicating the p:q rotation number (as explained in the *Rotation Number and Arnold Tongue* section) resulting from the stimulation parameters at that point, where 1:1 entrainment is in red and 1:2 entrainment is in blue-green. For both these panels, the black line indicates the 130Hz stimulation condition used in [6, 15]. (A) The sine circle map entrainment field for variable stimulation frequency with a fixed natural frequency of 75Hz. (B) The entrainment field of the Wilson-Cowan model with the top ranked parameters. The stimulation applied is a single time step pulse with no recharge. (C-D) The maximum height of the entrained peaks as predicted by the top-ranked Wilson-Cowan model fit, calculated as laid out in the *Providing Stimulation and Entrainment Analysis in the Model* section. Panel D is a magnified version of panel C (indicated by the grey rectangle) over stimulation parameter giving comparable results to panel E. (E) The height of entrained peaks for a series of different stimulation parameters. Circles display peak height of entrained parameters represented by the colour scale, while black triangles are for parameters that did not display entrainment (as can be seen in insert E2). The asterisk (*) by the unentrained point (150Hz, 6mA) indicates the presence of several changes in stimulation amplitude to the hemisphere not being studied during this recording, while the left hemisphere's stimulation parameters remained unchanged. 1:2 entrainment was not observed at any of these stimulation parameter sets. The occurrence of both a black triangle and a circle at the point (150Hz, 2.5mA) indicate intermittent entrainment, hence, this will likely be on the boundary of the tongue. Inserts E1-3 show PSDs over frequencies 60-80Hz.

decrease in power due to the aperiodic component of the power spectrum. Additionally, both the data and model show a small decrease in power with increased amplitude. Across the 130Hz stimulation frequency line we can observe a small but continual drop in the peak height as stimulation amplitude increases, as shown in Fig 5E.

Discussion

We show that the simplest model of a single neural oscillator with periodic stimulation, the sine circle map, is able to recreate the observation of 1:2 entrainment for cortical finely-tuned gamma oscillations (approximately 75Hz) to DBS at 130Hz in PD patients. The sine circle map represents a simple method to gain intuition of the response of a specific rhythm to stimulation, but it cannot be fitted to patient data. Through fitting a model of interacting neuronal populations to off-stimulation data, we are able to predict the region of stimulation parameters (frequency and amplitude) for which 1:2 entrainment is possible for this specific patient. In particular, our model predicts that 1:2 entrainment is lost in this patient when stimulation amplitude is increased beyond a certain value. Furthermore, the 1:2 Arnold tongue is left leaning, where 1:2 entrainment can be achieved for stimulation frequencies markedly lower than twice the frequency of the natural gamma rhythm. Lastly, the model further predicts that there would be a greater entrained gamma power at lower stimulation frequencies. Data recorded during therapeutic neurostimulation, after the modelling results were obtained, appeared to show 1:2 Arnold tongues that validate these predictions. Hence, the model can capture a range of sub-harmonic entrainment features without being constrained by entrainment data. This makes the model a good candidate for further investigations into the effects of high-frequency DBS on finely-tuned gamma in PD.

By solely analysing the presence of 1:2 entrainment, we avoid the prominent artefact at stimulation frequency. Hence, this analysis of the data provides a valuable, uncorrupted insight into the neuronal responses to stimulation. Bounding the 1:2 tongue for 150Hz stimulation, as we 'lose' 1:2 entrainment at increased stimulation amplitudes, also provides further evidence that the gamma peak at half stimulation frequency is not artefactual. This is aligned with the model prediction that 1:2 entrainment will be 'lost' when amplitude is increased beyond a certain point. Additionally, the model predicts that parameter changes that result in the 'loss' of 1:2 entrainment would see a transition to 1:1 entrainment. However, the presence of 1:1 entrainment is difficult to assess as the resulting power spectral peak can be masked by the stimulation artefact. In contrast, 1:2 entrainment does not suffer from this issue remaining free of stimulation artefact, which could provide a utility of sub-harmonic entrainment as a mechanism for accurate adaptive DBS [6] without having to remove stimulation artefact from a signal

containing the biomarker of interest. Furthermore, entrainment in the gamma frequency band has been linked with dyskinesia [6], showing that the entrained signal could be of clinical relevance.

The observation of the highest spectral peaks occurring at the lowest frequencies of stimulation may be somewhat counter-intuitive, since one could expect more stimulation energy to provide more oscillatory power. However, due to the increased time between successive pulses of stimulation at lower frequencies, the trajectory of the population activity covers a larger distance in phase space (see Supplementary Data section 2.4, specifically Supplementary Data Fig 2.4 for more details on population activity vector fields and trajectories). This means that the range of values that activity reaches for each population is greater, producing a higher power spectral peak for the given resultant frequency. Population activity having a larger range can also be interpreted as there being greater synchrony of neurons within the populations, as increased peak firing rates and decreased minima suggest more neurons are firing together.

1:2 entrainment is not an intrinsic property of the Wilson-Cowan model (large regions of parameter space do not lead to 1:2 entrainment). Additionally, if the parameters of the Wilson-Cowan model do produce 1:2 entrainment, the 1:2 tongue can also be right leaning or symmetrical about the central frequency, similar to the 1:2 tongue observed in the sine circle map (Fig 5A). Hence, the parameters of the Wilson-Cowan model need to be tuned to reproduce the data. Among the top-ranked Wilson-Cowan fits, there is some variability between the parameter sets and the corresponding entrainment predictions (see Supplementary Data section 2.1). This demonstrates that the model parameters are non-identifiable. However, as the best fits converge on results that all include a left leaning 1:2 tongue and given the validation of some of the model predictions by follow-up recordings, we can conclude that the fitted model remains a good candidate to make predictions for future investigations. It would be possible to fit Wilson-Cowan model parameters to on-stimulation entrainment data, which may or may not reproduce off-stimulation data. This is not something we are investigating as more value is provided by predicting the response from off-stimulation fits.

While only 1:2 entrainment is investigated here, entrainment will occur at other sub-harmonics of stimulation if there is a neuronal rhythm present to entrain and the corresponding tongue is large enough to encompass the neuronal rhythm. Similarly to 1:2 entrainment, sub-harmonic entrainment at every harmonic of stimulation is not an intrinsic property of Wilson-Cowan models. However, other sub-harmonic entrainment ratios can be observed for certain model parameter sets. Stimulating in the range of 130-160Hz in the patient, only 1:2 entrainment was explored for a 75Hz natural rhythm. By increasing stimulation frequency, for example to around 225Hz, it would be possible to investigate other sub-harmonic entrainment ratios such as 1:3 entrainment of this rhythm.

Study Limitations

As a case study, our approach has only been tested in one patient. Our patient-specific approach consists of fitting a neural mass model to off-stimulation data to predict stimulation parameters that will lead to 1:2 entrainment. In our case study, patient-specific predictions have been validated with follow-up recordings. However, it is unclear to what extent these predictions (such as the lean of the tongue) would generalise to other patients. We expect some variability in entrainment characteristics across patients, which further motivates a patient-specific approach. The extent of this variability is however unknown. Additionally, due to the limited amount of data obtained from this patient, it was not possible to perform a statistical analysis on the observations of 1:2 entrainment in response to variable stimulation parameters. Statistical analysis could have been achieved by repeating the observations across stimulation parameters several times, but this would not have been tolerated by this patient. Nevertheless, this case-study demonstrates the potential for a patient-specific approach to predict nonlinear effects of brain stimulation.

Furthermore, the stimulation parameters explored in this case study would benefit from a systematic mapping of the tongue boundary, with large regions of untested parameters and no full boundary being charted. Both of these shortcomings will be the focus of further investigations into 1:2 entrainment. However, extensive mapping of the tongue boundary may be limited by patient discomfort as some parameters tested are subtherapeutic and thus lead to brief exacerbation of motor signs.

Given that ECoG data represents the activity of populations of neurons, the Wilson-Cowan model is a good choice for this type of data. However, this doesn't allow us to observe or model the behaviour of individual neurons in response to stimulation and during 1:2 entrainment. Our approach is nonetheless adequate to predict stimulation parameters leading to 1:2 entrainment. Additionally, we have not included a population to represent the basal ganglia in our model. This was because there was no subcortical peak to fit a Wilson-Cowan network to for this patient. Subcortical narrowband oscillations in the basal ganglia have been recorded in long term recordings in other patients [8].

Implications

Throughout this study, it is demonstrated that brain rhythms can have nonlinear responses to stimulation, such as entrainment at harmonics of stimulation frequency, and non-monotonic rhythmic responses to amplitude. We argue against the simple view that only brain rhythms close to the stimulation frequency can be entrained (through 1:1 entrainment). The study also shows that if a specific entrainment ratio is observed at given stimulation parameters, increasing stimulation amplitude will not necessarily promote that corresponding frequency even further.

Given that entrainment to periodic stimulation has been observed in different frequency bands, our findings might have implications across frequencies. For instance, 1:1 entrainment has been reported in the alpha band through single pulse transcranial magnetic stimulation when treating depression [18], with rhythmic visual stimulation [19], and with tACS [38]. If rhythms can lock to harmonics of stimulation frequency, as supported by this study, it is possible that current stimulation protocols targeting any frequency band could induce unexpected responses at sub- or supra-harmonics of the stimulation frequency. Furthermore, when designing stimulation protocols one should be aware of potential ramifications of stimulation on other neuronal rhythms. For instance, stimulation targeting lower frequency oscillations, such as beta rhythms, may be able to entrain gamma at a 2:1 rotation number, or even alpha at a 1:2 rotation number. Similar considerations have been employed when designing stimulation protocols in a canine with epilepsy [39]. Our patient-specific approach can help predict these nonlinear responses. This is important since reinforcing oscillations at sub- or supra-harmonics might induce undesirable effects, or otherwise interfere with the therapeutic effect of stimulation.

Conclusion

We show that for certain network parameters, simple neural circuits can support 1:2 entrainment to DBS. In particular, our fitted Wilson-Cowan model provides theoretical evidence for a neural circuit origin of 1:2 entrainment of cortical gamma oscillation to high-frequency DBS in PD patients. Furthermore, it predicts a larger region of stimulation parameters, at frequencies corresponding to less than twice the natural frequency of the system, for which 1:2 entrainment would be observed. These results are validated by initial 1:2 entrainment charting from the same patient to whom the model was fitted.

Understanding the variety of effects of stimulation on various brain rhythms would provide valuable insights into designing stimulation protocols to provide maximum therapeutic benefit with minimal side effects. This model provides a first step to predicting these responses. Computational models enable us to experiment with a variety of waveforms without the burdensome tests and validation that would be associated with in patient trials. Prediction of the neuronal responses to stimulation is a fundamental step in the design of future therapeutic protocols. Our model predicts that these responses are not a simple one-for-one mapping of stimulation frequency and amplitudes to brain network activity and that stimulation may have significant effects, even when the stimulation frequency is outside of the frequency band of interest.

Supporting information

Supplementary Data Supplementary Appendix. Further details of the optimisation process, as well as the fitting robustness and entrainment predictions when different stimulation patterns are applied to the Wilson-Cowan model, are presented here.

Acknowledgements

The authors would like to acknowledge the use of the University of Oxford Advanced Research Computing (ARC) facility in carrying out this work. http://dx.doi.org/10.5281/zenodo.22558.

Data Availability

The data will be made available before publication.

Declaration of Competing Interest

PS receives research support from Medtronic Inc (providing investigational devices free of charge). SL is a scientific advisor for RuneLabs. The University of Oxford has research agreements with Bioinduction Ltd. TD has stock ownership (<1%) and business relationships with Bioinduction for research tool design and deployment, as well as being an advisor for Synchron and Cortec Neuro.

Funding Information

JS and TD are supported by DARPA HR0011- 20-2-0028 Manipulating and Optimizing Brain Rhythms for Enhancement of Sleep (Morpheus) and the UK Medical Research Council grant MC_UU_00003/3. MO and PS are supported by NIH/NINDS award R01NS090913. JA is supported by Swiss National Science Foundation (Early Postdoc Mobility – P2BEP3_188140). SL is supported by NIH award K23NS120037. RB and BD are supported by Medical Research Council grant MC_UU_00003/1. Content represents views of the authors and not the funders.

CRediT Author Statement

J.J. Sermon: Conceptualisation, Investigation, Methodology, Validation, Visualisation, Writing - original draft, Writing - review and editing. **M. Olaru:** Conceptualisation, Data Curation, Investigation, Writing - original draft, Writing - review and editing. **J. Anso:** Conceptualisation, Methodology,

Data Curation, Writing - review and editing. **S. Little:** Writing - review and editing. **R. Bogacz:** Conceptualisation, Funding Acquisition, Supervision, Writing - review and editing. **P.A. Starr:** Conceptualisation, Funding Acquisition, Resources, Supervision, Writing - review and editing. **T. Denison:** Conceptualisation, Funding Acquisition, Supervision, Writing - review and editing. **B. Duchet:** Conceptualisation, Investigation, Methodology, Supervision, Writing - review and editing.

References

[1] Conrado A. Bosman, Carien S. Lansink, and Cyriel M.A. Pennartz. Functions of gamma-band synchronization in cognition: From single circuits to functional diversity across cortical and subcortical systems. *European Journal of Neuroscience*, 39(11):1982–1999, jun 2014.

[2] Magdalena Nowak, Catharina Zich, and Charlotte J. Stagg. Motor Cortical Gamma Oscillations: What Have We Learnt and Where Are We Headed?, apr 2018.

[3] Michael Cassidy, Paolo Mazzone, Antonio Oliviero, Angelo Insola, Pietro Tonali, Vincenzo Di Lazzaro, and Peter Brown. Movement-related changes in synchronization in the human basal ganglia. *Brain*, 125(6):1235–1246, jun 2002.

[4] David Williams, Marina Tijssen, Gerard Van Bruggen, Andries Bosch, Angelo Insola, Vincenzo Di Lazzaro, Paolo Mazzone, Antonio Oliviero, Angelo Quartarone, Hans Speelman, and Peter Brown. Dopamine-dependent changes in the functional connectivity between basal ganglia and cerebral cortex in humans. *Brain*, 125(7):1558–1569, jul 2002.

[5] C. Wiest, F. Torrecillos, G. Tinkhauser, A. Pogosyan, F. Morgante, E.A. Pereira, and H. Tan. Finely-tuned gamma oscillations: Spectral characteristics and links to dyskinesia — Elsevier Enhanced Reader. *Experimental Neurology*, 351:113999, 2022.

[6] Nicole C. Swann, Coralie De Hemptinne, Svjetlana Miocinovic, Salman Qasim, Sarah S. Wang, Nathan Ziman, Jill L. Ostrem, Marta San Luciano, Nicholas B. Galifianakis, and Philip A. Starr. Gamma oscillations in the hyperkinetic state detected with chronic human brain recordings in parkinson's disease. *Journal of Neuroscience*, 36(24):6445–6458, jun 2016.

[7] Coralie de Hemptinne, Doris D. Wang, Svjetlana Miocinovic, Witney Chen, Jill L. Ostrem, and Philip A. Starr. Pallidal thermolesion unleashes gamma oscillations in the motor cortex in Parkinson's disease. *Movement Disorders*, 34(6):903–911, jun 2019.

[8] Ro'ee Gilron, Simon Little, Randy Perrone, Robert Wilt, Coralie de Hemptinne, Maria S. Yaroshinsky, Caroline A. Racine, Sarah S. Wang, Jill L. Ostrem, Paul S. Larson, Doris D. Wang, Nick B. Galifianakis, Ian O. Bledsoe, Marta San Luciano, Heather E. Dawes, Gregory A. Worrell, Vaclav Kremen, David A. Borton, Timothy Denison, and Philip A. Starr. Long-term wireless streaming of neural recordings for circuit discovery and adaptive stimulation in individuals with Parkinson's disease. *Nature Biotechnology*, 39(9):1078–1085, may 2021.

[9] Pär Halje, Martin Tamtè, Ulrike Richter, Mohsin Mohammed, M. Angela Cenci, and Per Petersson. Levodopa-induced dyskinesia is strongly associated with resonant cortical oscillations. *Journal of Neuroscience*, 32(47):16541–16551, nov 2012.

[10] Christopher Güttler, Jennifer Altschüler, Kaloyan Tanev, Saskia Böckmann, Jens Kersten Haumesser, Vadim V. Nikulin, Andrea A. Kühn, and Christoph van Riesen. Levodopa-Induced Dyskinesia Are Mediated by Cortical Gamma Oscillations in Experimental Parkinsonism. *Movement Disorders*, 36(4):927–937, apr 2021.

[11] E. W. Tsang, C. Hamani, E. Moro, F. Mazzella, U. Saha, A. M. Lozano, M. Hodaie, R. Chuang, T. Steeves, S. Y. Lim, B. Neagu, and R. Chen. Subthalamic deep brain stimulation at individualized frequencies for Parkinson disease. *Neurology*, 78(24):1930–1938, jun 2012.

[12] Andrea Guerra, Donato Colella, Margherita Giangrosso, Antonio Cannavacciuolo, Giulia Paparella, Giovanni Fabbrini, Antonio Suppa, Alfredo Berardelli, and Matteo Bologna. Driving motor cortex oscillations modulates bradykinesia in Parkinson's disease. *Brain*, jul 2021.

[13] Eric Lowet, Mark J. Roberts, Alina Peter, Bart Gips, and Peter De Weerd. A quantitative theory of gamma synchronization in macaque V1. *eLife*, 6, aug 2017.

[14] Muthuraman Muthuraman, Manuel Bange, Nabin Koirala, Dumitru Ciolac, Bogdan Pintea, Martin Glaser, Gerd Tinkhauser, Peter Brown, Gunther Deuschl, and Sergiu Groppa. Cross-frequency coupling between gamma oscillations and deep brain stimulation frequency in Parkinson's disease. *Brain*, 143(11):3393–3407, nov 2021.

[15] Nicole C. Swann, Coralie De Hemptinne, Margaret C. Thompson, Svjetlana Miocinovic, Andrew M. Miller, Ro'Ee Gilron, Jill L. Ostrem, Howard J. Chizeck, and Philip A. Starr. Adaptive deep brain stimulation for Parkinson's disease using motor cortex sensing. *Journal of Neural Engineering*, 15(4), may 2018.

[16] J. Anso, R. Gilron, M. Yaroshinsky, R. Wilt, R. Perrone, I. Bledsoe, M. San Luciano, J. Ostrem, S. Little, C. de Hemptinne, and P. Starr. 895 Pallidal deep brain stimulation entrains finely tuned gamma oscillations in motor cortex. *Movement Disorders Abstracts 2021: official journal of the Movement Disorder Society*, 36:S1–S599, sep 2021.

[17] V I Arnol'd. Remarks on the perturbation theory for problems of Mathieu type. *Russian Mathematical Surveys*, 38(4):215–233, aug 1983.

[18] Flavio Fröhlich. Tuning out the blues - Thalamo-cortical rhythms as a successful target for treating depression, nov 2015.

[19] Annika Notbohm, Jürgen Kurths, and Christoph S. Herrmann. Modification of brain oscillations via rhythmic light stimulation provides evidence for entrainment but not for superposition of event-related responses. *Frontiers in Human Neuroscience*, 10(FEB2016), feb 2016.

[20] Mohsin M. Ali, Kristin K. Sellers, and Flavio Fröhlich. Transcranial alternating current stimulation modulates large-scale cortical network activity by network resonance. *Journal of Neuroscience*, 33(27):11262–11275, jul 2013.

[21] Simon Hanslmayr, Nikolai Axmacher, and Cory S. Inman. Modulating Human Memory via Entrainment of Brain Oscillations, jul 2019.

[22] Hugh R. Wilson and Jack D. Cowan. Excitatory and Inhibitory Interactions in Localized Populations of Model Neurons. *Biophysical Journal*, 12(1):1–24, 1972.

[23] Jack D. Cowan, Jeremy Neuman, and Wim van Drongelen. Wilson–Cowan Equations for Neocortical Dynamics. *Journal of Mathematical Neuroscience*, 6(1):1–24, jan 2016.

[24] Caroline A. Lea-Carnall, Marcelo A. Montemurro, Nelson J. Trujillo-Barreto, Laura M. Parkes, and Wael El-Deredy. Cortical Resonance Frequencies Emerge from Network Size and Connectivity. *PLoS Computational Biology*, 12(2):e1004740, feb 2016.

[25] Osvaldo Matías Velarde, Germán Mato, and Damián Dellavale. Mechanisms for pattern specificity of deep-brain stimulation in Parkinson's disease. *PLoS ONE*, 12(8):e0182884, aug 2017.

[26] Vassilis Cutsuridis. *Multiscale Models of Brain Disorders*. 2019.

[27] Nada Yousif, Michael Mace, Nicola Pavese, Roman Borisyuk, Dipankar Nandi, and Peter Bain. A Network Model of Local Field Potential Activity in Essential Tremor and the Impact of Deep Brain Stimulation. *PLoS Computational Biology*, 13(1):e1005326, jan 2017.

[28] Benoit Duchet, Gihan Weerasinghe, Hayriye Cagnan, Peter Brown, Christian Bick, and Rafal Bogacz. Phase-dependence of response curves to deep brain stimulation and their relationship: from essential tremor patient data to a Wilson–Cowan model. *Journal of Mathematical Neuroscience*, 10(1), dec 2020.

[29] Alberto Pérez-Cervera, Tere M-Seara, and Gemma Huguet. A Geometric Approach to Phase Response Curves and Its Numerical Computation Through the Parameterization Method. *Journal of Nonlinear Science*, 29(6):2877–2910, sep 2019.

[30] Christoforos A. Papasavvas, Andrew J. Trevelyan, Marcus Kaiser, and Yujiang Wang. Divisive gain modulation enables flexible and rapid entrainment in a neocortical microcircuit model. *Journal of Neurophysiology*, 123(3):1133–1143, mar 2020.

[31] Romain Veltz and Terrence J. Sejnowski. Periodic forcing of inhibition-stabilized networks: Nonlinear resonances and phase-amplitude coupling. *Neural Computation*, 27(12):2477–2509, dec 2015.

[32] Frank C. Hoppensteadt and Eugene M. Izhikevich. Thalamo-cortical interactions modeled by weakly connected oscillators: Could the brain use FM radio principles? In *BioSystems*, volume 48, pages 85–94. Biosystems, nov 1998.

[33] Roman M. Borisyuk and Alexandr B. Kirillov. Bifurcation analysis of a neural network model. *Biological Cybernetics*, 66(4):319–325, feb 1992.

[34] Angela C.E. Onslow, Matthew W. Jones, and Rafal Bogacz. A canonical circuit for generating phase-amplitude coupling. *PLoS ONE*, 9(8):e102591, aug 2014.

[35] Paolo Calabresi, Barbara Picconi, Alessandro Tozzi, Veronica Ghiglieri, and Massimiliano Di Filippo. Direct and indirect pathways of basal ganglia: A critical reappraisal, 2014.

[36] Jie Dong, Sarah Hawes, Junbing Wu, Weidong Le, and Huaibin Cai. Connectivity and Functionality of the Globus Pallidus Externa Under Normal Conditions and Parkinson's Disease, mar 2021.

[37] Benoit Duchet, Filippo Ghezzi, Gihan Weerasinghe, Gerd Tinkhauser, A. A. Kühn, Peter Brown, Christian Bick, and Rafal Bogacz. Average beta burst duration profiles provide a signature of dynamical changes between the on and off medication states in Parkinson's disease. *PLoS Computational Biology*, 17(7):e1009116, jul 2021.

[38] Wei A. Huang, Iain M. Stitt, Ehsan Negahbani, D. J. Passey, Sangtae Ahn, Marshall Davey, Moritz Dannhauer, Thien T. Doan, Anna C. Hoover, Angel V. Peterchev, Susanne Radtke-Schuller, and Flavio Fröhlich. Transcranial alternating current stimulation entrains alpha oscillations by preferential phase synchronization of fast-spiking cortical neurons to stimulation waveform. *Nature Communications*, 12(1):1–20, may 2021.

[39] Mayela Zamora, Sebastian Meller, Filip Kajin, James J. Sermon, Robert Toth, Moaad Benjaber, Derk-Jan Dijk, Rafal Bogacz, Gregory A. Worrell, Antonio Valentin, Benoit Duchet, Holger A. Volk, and Timothy Denison. Case Report: Embedding "Digital Chronotherapy" Into Medical

Devices—A Canine Validation for Controlling Status Epilepticus Through Multi-Scale Rhythmic Brain Stimulation. *Frontiers in Neuroscience*, 15:1196, sep 2021.